

hep-ph/0107159
July 2001

New physics signatures at a Linear Collider: model-independent analysis from ‘conventional’ polarized observables

A.A. Babich^a, P. Osland^b, A.A. Pankov^{a,c,d} and N. Paver^c

^a Pavel Sukhoi Technical University, Gomel, 246746 Belarus

^b Department of Physics, University of Bergen,
Allégaten 55, N-5007 Bergen, Norway

^c Dipartimento di Fisica Teorica, Università di Trieste and
Istituto Nazionale di Fisica Nucleare, Sezione di Trieste, Trieste, Italy

^d The Abdus Salam International Centre for Theoretical Physics, Trieste, Italy

Abstract

We discuss four-fermion contact-interaction searches in the processes $e^+e^- \rightarrow \mu^+\mu^-$, $c\bar{c}$ and $b\bar{b}$ at a future e^+e^- Linear Collider with c.m. energy $\sqrt{s} = 0.5$ TeV and with both beams longitudinally polarized. Our analysis is based on the measurements of familiar polarized observables such as the total cross section and the forward-backward/left-right asymmetries, and accounts for the general set of contact interaction couplings as independent, non-zero, parameters thus avoiding simplifying, model-dependent, assumptions. We derive the corresponding model-independent constraints on the above-mentioned coupling constants, and evaluate the corresponding reach at the Linear Collider, emphasizing the role of beam polarization. We compare the results with a model-dependent procedure where only one coupling is varied at a time.

1 Introduction

Contact interaction Lagrangians (CI) generally represent an effective description of the ‘low energy’ manifestations of some non-standard dynamics acting at new, intrinsic, mass scales much higher than the energies reachable at current particle accelerators. As such, they can be studied through deviations of the experimental observables from the Standard Model (SM) expectation, that reflect the additional presence of the above-mentioned new interaction. Typical examples are the composite models and the exchanges of extremely heavy neutral gauge bosons and leptoquarks [1, 2].

Clearly, such deviations are expected to be extremely small, as they would be suppressed for dimensional reasons by essentially some power of the ratio between the available energy and the large mass scales. Accordingly, very high energy reactions in experiments with high luminosity are one of the natural tools to investigate signatures of contact interaction couplings. In general, these constants are considered as *a priori* free parameters, and one can quantitatively derive an assessment of the attainable reach and of the corresponding upper limits, essentially by numerically comparing the deviations with the expected experimental statistical and systematical uncertainties on the cross sections.

Here, we consider the fermion pair production process

$$e^+ + e^- \rightarrow f + \bar{f}, \quad (1)$$

with $f \neq e, t$, at a Linear Collider (LC) with c.m. energy $\sqrt{s} = 0.5 \text{ TeV}$ and polarized electron and positron beams. We discuss the sensitivity of this reaction to the general, $SU(3) \times SU(2) \times U(1)$ symmetric $eeff$ contact-interaction effective Lagrangian, with helicity-conserving and flavor-diagonal fermion currents [3]:

$$\mathcal{L}_{\text{CI}} = \sum_{\alpha\beta} g_{\text{eff}}^2 \epsilon_{\alpha\beta} (\bar{e}_\alpha \gamma_\mu e_\alpha) (\bar{f}_\beta \gamma^\mu f_\beta). \quad (2)$$

In Eq. (2): $\alpha, \beta = L, R$ denote left- or right-handed helicities, generation and color indices have been suppressed, and the CI coupling constants are parameterized in terms of corresponding mass scales as $\epsilon_{\alpha\beta} = \eta_{\alpha\beta}/\Lambda_{\alpha\beta}^2$ with $\eta_{\alpha\beta} = \pm 1, 0$ depending on the chiral structure of the individual interactions. Also, conventionally the value of g_{eff}^2 is fixed at $g_{\text{eff}}^2 = 4\pi$, as a reminder that, in the case of compositeness, the new interaction would become strong at \sqrt{s} of the order of $\Lambda_{\alpha\beta}$. Obviously, in this parameterization, exclusion ranges or upper limits on the CI couplings can be equivalently expressed as exclusion ranges or lower bounds on the corresponding mass scales $\Lambda_{\alpha\beta}$.

For a given final fermion flavor f , \mathcal{L}_{CI} in Eq. (2) envisages the existence of eight individual, and independent, CI models corresponding to the combinations of the four chiralities α, β with the \pm signs of the η ’s, with *a priori* free, and nonvanishing, coefficients. Correspondingly, the most general (and model-independent) analysis of the process (1) must account for the complicated situation where all four-fermion effective couplings defined in Eq. (2) are simultaneously allowed in the expression for the cross section, and in principle can interfere and weaken the bounds in case of accidental cancellations.

Of course, the different helicity amplitudes, as such, do not interfere. However, *the deviations from the SM* could be positive for one helicity amplitude, and negative for another. Thus, cancellations might occur.

The simplest attitude is to assume non-zero values for only one of the couplings (or one specific combination of them) at a time, with all others zero, this leads to tests of the specific models mentioned above. Currently, such models for lepton-lepton and lepton-quark contact interactions are constrained along this line, for the different flavours, by experiments on lepton and hadron production in e^+e^- annihilation, unpolarized and polarized deep inelastic scattering, production of Drell-Yan lepton pairs, and atomic parity violation, see, e.g., Refs. [1] and [4–7]. Global analyses are often performed for individual lepton-quark CI’s, by combining data from various experiments and processes relevant to the same kind of coupling. The resulting bounds on Λ ’s are quite sensitive to the particular one-parameter scenario considered in the analysis of the data and, without entering into details, typically range between 5 and 12 TeV.

On the other hand, in principle, constraints obtained by simultaneously including couplings of different chiralities might become considerably weaker, as noted above and also in Ref. [6]. Therefore, it should be highly desirable to apply a more general (and model-independent) approach to the analysis of experimental data, that simultaneously includes all terms of Eq. (2) as independent free parameters, and can also allow the derivation of separate constraints (or exclusion regions) on the values of the coupling constants.

To this aim, in the case of the process (1) at the LC considered here, a possibility is offered by initial beam polarization, that enables us to extract from the data the individual helicity cross sections through the definition of particular, and optimal, polarized integrated cross sections and, consequently, to disentangle the constraints on the corresponding CI constants [8–11]. In this article, we wish to present a model-independent analysis of the CI that complements that of Refs. [8–11], and is based instead on the measurements of more ‘conventional’ observables (but still assuming polarized electron and positron beams) such as the total cross section, the forward-backward asymmetry A_{FB} , the left-right asymmetry A_{LR} , and left-right forward-backward asymmetry $A_{LR,FB}$. A particularly delicate point in the derivation of bounds is, in this case, the correlation among uncertainties on the different observables, that will be taken into account *via* the method of the covariance matrix.

The remainder of the paper is organized as follows. In Sect. 2 we discuss the observables being considered, which are the conventional observables, as opposed to the more delicate optimal observables considered elsewhere [9–11]. In Sect. 3 we present an error analysis together with the numerical input and the resulting bounds on contact-interaction parameters.

2 Observables

For the process Eq. (1), limiting ourselves to the cases $f \neq e, t$, we can neglect fermion masses with respect to \sqrt{s} , and express the amplitude in the Born approximation including the γ and Z s -channel exchanges plus the contact-interaction term of Eq. (2). With P_e

and $P_{\bar{e}}$ the longitudinal polarizations of the electron and positron beams, respectively, and θ the angle between the incoming electron and the outgoing fermion in the c.m. frame, the differential cross section can be expressed as [12]:

$$\frac{d\sigma}{d\cos\theta} = \frac{3}{8} [(1 + \cos\theta)^2 \sigma_+ + (1 - \cos\theta)^2 \sigma_-]. \quad (3)$$

In terms of the helicity cross sections $\sigma_{\alpha\beta}$ (with $\alpha, \beta = L, R$), directly related to the individual CI couplings $\epsilon_{\alpha\beta}$:

$$\begin{aligned} \sigma_+ &= \frac{1}{4} [(1 - P_e)(1 + P_{\bar{e}}) \sigma_{LL} + (1 + P_e)(1 - P_{\bar{e}}) \sigma_{RR}] \\ &= \frac{D}{4} [(1 - P_{\text{eff}}) \sigma_{LL} + (1 + P_{\text{eff}}) \sigma_{RR}], \end{aligned} \quad (4)$$

$$\begin{aligned} \sigma_- &= \frac{1}{4} [(1 - P_e)(1 + P_{\bar{e}}) \sigma_{LR} + (1 + P_e)(1 - P_{\bar{e}}) \sigma_{RL}] \\ &= \frac{D}{4} [(1 - P_{\text{eff}}) \sigma_{LR} + (1 + P_{\text{eff}}) \sigma_{RL}], \end{aligned} \quad (5)$$

where

$$P_{\text{eff}} = \frac{P_e - P_{\bar{e}}}{1 - P_e P_{\bar{e}}} \quad (6)$$

is the effective polarization [13], $|P_{\text{eff}}| \leq 1$, and $D = 1 - P_e P_{\bar{e}}$. For unpolarized positrons $P_{\text{eff}} \rightarrow P_e$ and $D \rightarrow 1$, but with $P_{\bar{e}} \neq 0$, $|P_{\text{eff}}|$ can be larger than $|P_e|$. Moreover, in Eqs. (4) and (5):

$$\sigma_{\alpha\beta} = N_C \sigma_{\text{pt}} |\mathcal{M}_{\alpha\beta}|^2, \quad (7)$$

where $N_C \approx 3(1 + \alpha_s/\pi)$ for quarks and $N_C = 1$ for leptons, respectively, and $\sigma_{\text{pt}} \equiv \sigma(e^+ e^- \rightarrow \gamma^* \rightarrow l^+ l^-) = (4\pi\alpha^2)/(3s)$. The helicity amplitudes $\mathcal{M}_{\alpha\beta}$ can be written as

$$\mathcal{M}_{\alpha\beta} = Q_e Q_f + g_{\alpha}^e g_{\beta}^f \chi_Z + \frac{s}{\alpha} \epsilon_{\alpha\beta} \quad (8)$$

where $\chi_Z = s/(s - M_Z^2 + iM_Z\Gamma_Z)$ represents the Z propagator, $g_L^f = (I_{3L}^f - Q_f s_W^2)/s_W c_W$ and $g_R^f = -Q_f s_W^2/s_W c_W$ are the SM left- and right-handed fermion couplings of the Z with $s_W^2 = 1 - c_W^2 \equiv \sin^2 \theta_W$ and Q_f the fermion electric charge.

We now define, with ϵ the experimental efficiency for detecting the final state under consideration, the four, directly measurable, integrated event rates:

$$N_{L,F}, \quad N_{R,F}, \quad N_{L,B}, \quad N_{R,B}, \quad (9)$$

where ($\alpha = L, R$)

$$N_{\alpha,F} = \frac{1}{2} \mathcal{L}_{\text{int}} \epsilon \int_0^1 (d\sigma_{\alpha}/d\cos\theta) d\cos\theta, \quad (10)$$

$$N_{\alpha,B} = \frac{1}{2} \mathcal{L}_{\text{int}} \epsilon \int_{-1}^0 (\text{d}\sigma_\alpha / \text{d}\cos\theta) \text{d}\cos\theta, \quad (11)$$

and subscripts R and L correspond to two sets of beam polarizations, $P_e = +P_1$, $P_{\bar{e}} = -P_2$ ($P_{1,2} > 0$) and $P_e = -P_1$, $P_{\bar{e}} = +P_2$, respectively, or, alternatively, $P_{\text{eff}} = \pm P$ with D fixed. In Eqs. (10) and (11), \mathcal{L}_{int} is the time-integrated luminosity, we assume it to be equally distributed over the two combinations of beam polarizations, L and R.

The set of ‘conventional’ observables we consider here for the discussion of bounds on the CI parameters are the unpolarized cross section:

$$\sigma_{\text{unpol}} = \frac{1}{4} [\sigma_{\text{LL}} + \sigma_{\text{LR}} + \sigma_{\text{RR}} + \sigma_{\text{RL}}]; \quad (12)$$

the (unpolarized) forward-backward asymmetry:

$$A_{\text{FB}} = \frac{3}{4} \frac{\sigma_{\text{LL}} - \sigma_{\text{LR}} + \sigma_{\text{RR}} - \sigma_{\text{RL}}}{\sigma_{\text{LL}} + \sigma_{\text{LR}} + \sigma_{\text{RR}} + \sigma_{\text{RL}}}; \quad (13)$$

the left-right and the left-right forward-backward asymmetries (which both require polarization), that can be written as, respectively:

$$A_{\text{LR}} = \frac{\sigma_{\text{LL}} + \sigma_{\text{LR}} - \sigma_{\text{RR}} - \sigma_{\text{RL}}}{\sigma_{\text{LL}} + \sigma_{\text{LR}} + \sigma_{\text{RR}} + \sigma_{\text{RL}}}, \quad (14)$$

and

$$A_{\text{LR,FB}} = \frac{3}{4} \frac{\sigma_{\text{LL}} - \sigma_{\text{RR}} + \sigma_{\text{RL}} - \sigma_{\text{LR}}}{\sigma_{\text{LL}} + \sigma_{\text{RR}} + \sigma_{\text{RL}} + \sigma_{\text{LR}}}. \quad (15)$$

Using Eqs. (7) and (8), one can easily express the deviations of these observables from the SM predictions in terms of the SM couplings and the CI couplings $\epsilon_{\alpha\beta}$ of Eq. (2).

The above observables are connected to the measured ones through the integrated event rates $N_{\text{L,R;F,B}}$, see Eq. (9), as follows:

$$D \sigma_{\text{unpol}} = \frac{N_{\text{tot}}^{\text{exp}}}{\mathcal{L}_{\text{int}} \epsilon}, \quad (16)$$

where

$$N_{\text{tot}}^{\text{exp}} = N_{\text{L,F}} + N_{\text{R,F}} + N_{\text{L,B}} + N_{\text{R,B}} \quad (17)$$

is the total number of events observed with polarized beams (for the four measurements). Eq. (16) expresses the well-known fact that, when both the electron and positron beams are polarized, the total annihilation cross section into fermion-antifermion pairs will be increased by the factor D , with $1 \leq D \leq 2$.

For the experimental forward-backward asymmetry:

$$A_{\text{FB}} = A_{\text{FB}}^{\text{exp}} \equiv \frac{N_{\text{L,F}} + N_{\text{R,F}} - N_{\text{L,B}} - N_{\text{R,B}}}{N_{\text{L,F}} + N_{\text{R,F}} + N_{\text{L,B}} + N_{\text{R,B}}}, \quad (18)$$

Finally, for the experimental left-right and left-right forward-backward asymmetries the relations are

$$P_{\text{eff}} A_{\text{LR}} = A_{\text{LR}}^{\text{exp}} \equiv \frac{N_{\text{L,F}} + N_{\text{L,B}} - N_{\text{R,F}} - N_{\text{R,B}}}{N_{\text{L,F}} + N_{\text{L,B}} + N_{\text{R,F}} + N_{\text{R,B}}}, \quad (19)$$

and

$$P_{\text{eff}} A_{\text{LR,FB}} = A_{\text{LR,FB}}^{\text{exp}} \equiv \frac{(N_{\text{L,F}} - N_{\text{R,F}}) - (N_{\text{L,B}} - N_{\text{R,B}})}{N_{\text{L,F}} + N_{\text{R,F}} + N_{\text{L,B}} + N_{\text{R,B}}}. \quad (20)$$

In the following analysis, cross sections will be evaluated including initial- and final-state radiation by means of the program ZFITTER [14], which has to be used along with ZEFT, adapted to the present discussion, with $m_{\text{top}} = 175$ GeV and $m_H = 120$ GeV. One-loop SM electroweak corrections are accounted for by improved Born amplitudes [15, 16], such that the forms of the previous formulae remain the same. Concerning initial-state radiation, a cut on the energy of the emitted photon $\Delta = E_{\gamma}/E_{\text{beam}} = 0.9$ is applied for $\sqrt{s} = 0.5$ TeV in order to avoid the radiative return to the Z peak, and increase the signal originating from the contact interaction contribution [17].

As numerical inputs, we shall assume the commonly used reference values of the identification efficiencies [18]: $\epsilon = 95\%$ for l^+l^- ; $\epsilon = 60\%$ for $b\bar{b}$; $\epsilon = 35\%$ for $c\bar{c}$. Concerning the statistical uncertainty, to study the relative roles of statistical and systematic uncertainties we shall vary \mathcal{L}_{int} from 50 to 500 fb^{-1} (half for each polarization orientation) with uncertainty $\delta\mathcal{L}_{\text{int}}/\mathcal{L}_{\text{int}} = 0.5\%$, and a fiducial experimental angular range $|\cos\theta| \leq 0.99$. Also, regarding electron and positron degrees of polarization, we shall consider the values: $|P_e| = 0.8$; $|P_{\bar{e}}| = 0.0, 0.4$ and 0.6 , with $\delta P_e/P_e = \delta P_{\bar{e}}/P_{\bar{e}} = 0.5\%$.

3 Numerical analysis and constraints on CI couplings

The current bounds on $\Lambda_{\alpha\beta}$ cited in Sect. 1, of the order of several TeV, are such that for the LC c.m. energy $\sqrt{s} = 0.5$ TeV the characteristic suppression factor s/Λ^2 in Eq. (8) is rather strong. Accordingly, we can safely assume a linear dependence of the cross sections on the parameters $\epsilon_{\alpha\beta}$. In this regard, indirect manifestations of the CI interaction (2) can be looked for, *via* deviations of the measured observables from the SM predictions, caused by the new interaction. The reach on the CI couplings, and the corresponding constraints on their allowed values in the case of no effect observed, can be estimated by comparing the expression of the mentioned deviations with the expected experimental (statistical and systematic) uncertainties.

To this purpose, assuming the data to be well described by the SM ($\epsilon_{\alpha\beta} = 0$) predictions, i.e., that no deviation is observed within the foreseen experimental uncertainty, and in the linear approximation in $\epsilon_{\alpha\beta}$ of the observables (12)–(15), we apply the method based on the covariance matrix:

$$V_{kl} = \langle (\mathcal{O}_k - \bar{\mathcal{O}}_k)(\mathcal{O}_l - \bar{\mathcal{O}}_l) \rangle$$

$$\begin{aligned}
&= \sum_{i=1}^4 (\delta N_i)^2 \left(\frac{\partial \mathcal{O}_k}{\partial N_i} \right) \left(\frac{\partial \mathcal{O}_l}{\partial N_i} \right) + (\delta \mathcal{L}_{\text{int}})^2 \left(\frac{\partial \mathcal{O}_k}{\partial \mathcal{L}_{\text{int}}} \right) \left(\frac{\partial \mathcal{O}_l}{\partial \mathcal{L}_{\text{int}}} \right) \\
&+ (\delta P_e)^2 \left(\frac{\partial \mathcal{O}_k}{\partial P_e} \right) \left(\frac{\partial \mathcal{O}_l}{\partial P_e} \right) + (\delta P_{\bar{e}})^2 \left(\frac{\partial \mathcal{O}_k}{\partial P_{\bar{e}}} \right) \left(\frac{\partial \mathcal{O}_l}{\partial P_{\bar{e}}} \right). \tag{21}
\end{aligned}$$

Here, the N_i are given by Eq. (9), so that the statistical error appearing on the right-hand-side is given by

$$\delta N_i = \sqrt{N_i}, \tag{22}$$

and the $\mathcal{O}_l = (\sigma_{\text{unpol}}, A_{\text{FB}}, A_{\text{LR}}, A_{\text{LR,FB}})$ are the four observables. The second, third and fourth terms of the right-hand-side of Eq. (21) represent the systematic errors on the integrated luminosity \mathcal{L}_{int} , polarizations P_e and $P_{\bar{e}}$, respectively, for which we assume the numerical values reported in the previous Section. From the explicit expression of the matrix elements V_{kl} , one can easily notice that, apart from σ_{unpol} and A_{FB} that are uncorrelated ($V_{12} = 0$), all other pairs of observables show a correlation. Indeed, the non-zero diagonal entries are given by:

$$\begin{aligned}
V_{11} &= \frac{\sigma_{\text{unpol}}^2}{N_{\text{tot}}^{\text{exp}}} + \sigma_{\text{unpol}}^2 \left[\frac{P_e^2 P_{\bar{e}}^2}{D^2} (\epsilon_e^2 + \epsilon_{\bar{e}}^2) + \epsilon_{\mathcal{L}}^2 \right]; & V_{22} &= \frac{1 - A_{\text{FB}}^2}{N_{\text{tot}}^{\text{exp}}}, \\
V_{33} &= \frac{1 - A_{\text{LR}}^2 P_{\text{eff}}^2}{P_{\text{eff}}^2 N_{\text{tot}}^{\text{exp}}} + A_{\text{LR}}^2 \Delta_2^2; & V_{44} &= \frac{1 - A_{\text{LR,FB}}^2 P_{\text{eff}}^2}{P_{\text{eff}}^2 N_{\text{tot}}^{\text{exp}}} + A_{\text{LR,FB}}^2 \Delta_2^2, \tag{23}
\end{aligned}$$

and, for the non-diagonal ones we have:

$$\begin{aligned}
V_{13} &= \sigma_{\text{unpol}} A_{\text{LR}} \Delta_1^2; & V_{14} &= \sigma_{\text{unpol}} A_{\text{LR,FB}} \Delta_1^2; & V_{23} &= \frac{A_{\text{LR,FB}} - A_{\text{FB}} A_{\text{LR}}}{N_{\text{tot}}^{\text{exp}}}, \\
V_{24} &= \frac{A_{\text{LR}} - A_{\text{FB}} A_{\text{LR,FB}}}{N_{\text{tot}}^{\text{exp}}}; & V_{34} &= \frac{A_{\text{FB}} - A_{\text{LR}} A_{\text{LR,FB}} P_{\text{eff}}^2}{P_{\text{eff}}^2 N_{\text{tot}}^{\text{exp}}} + A_{\text{LR}} A_{\text{LR,FB}} \Delta_2^2. \tag{24}
\end{aligned}$$

Here:

$$\begin{aligned}
\Delta_1^2 &= \frac{P_e P_{\bar{e}}}{P_{\text{eff}} D^3} \left[-(1 - P_{\bar{e}}^2) P_e \epsilon_e^2 + (1 - P_e^2) P_{\bar{e}} \epsilon_{\bar{e}}^2 \right], \\
\Delta_2^2 &= \frac{(1 - P_{\bar{e}}^2)^2 P_e^2 \epsilon_e^2 + (1 - P_e^2)^2 P_{\bar{e}}^2 \epsilon_{\bar{e}}^2}{P_{\text{eff}}^2 D^4}, \tag{25}
\end{aligned}$$

and $\epsilon_e = \delta P_e / P_e$, $\epsilon_{\bar{e}} = \delta P_{\bar{e}} / P_{\bar{e}}$ and $\epsilon_{\mathcal{L}} = \delta \mathcal{L}_{\text{int}} / \mathcal{L}_{\text{int}}$ are the relative systematic uncertainties.

One can notice, from Eq. (23), that systematic uncertainties in σ_{unpol} are induced by ϵ_e , $\epsilon_{\bar{e}}$ and $\epsilon_{\mathcal{L}}$, while those in A_{LR} and $A_{\text{LR,FB}}$ arise from ϵ_e and $\epsilon_{\bar{e}}$ only, and *not* from $\epsilon_{\mathcal{L}}$. Finally, A_{FB} is free from such systematic uncertainties.

Defining the inverse covariance matrix W^{-1} as

$$(W^{-1})_{ij} = \sum_{k,l=1}^4 (V^{-1})_{kl} \left(\frac{\partial \mathcal{O}_k}{\partial \epsilon_i} \right) \left(\frac{\partial \mathcal{O}_l}{\partial \epsilon_j} \right), \tag{26}$$

with $\epsilon_i = (\epsilon_{LL}, \epsilon_{LR}, \epsilon_{RL}, \epsilon_{RR})$, model-independent allowed domains in the four-dimensional CI parameter space to 95% confidence level are obtained from the error contours determined by the quadratic form in $\epsilon_{\alpha\beta}$ [19, 20]:

$$(\epsilon_{LL} \ \epsilon_{LR} \ \epsilon_{RL} \ \epsilon_{RR}) W^{-1} \begin{pmatrix} \epsilon_{LL} \\ \epsilon_{LR} \\ \epsilon_{RL} \\ \epsilon_{RR} \end{pmatrix} = 9.49. \quad (27)$$

The value 9.49 on the right-hand side of Eq. (27) corresponds to a fit with four free parameters [21, 22].

The quadratic form (27) defines a four-dimensional ellipsoid in the $(\epsilon_{LL}, \epsilon_{LR}, \epsilon_{RL}, \epsilon_{RR})$ parameter space. The matrix W has the property that the square roots of the individual diagonal matrix elements, $\sqrt{W_{ii}}$, determine the projection of the ellipsoid onto the corresponding i -parameter axis in the four-dimensional space, and has the meaning of the bound at one σ on that parameter regardless of the values assumed for the others. Conversely, $1/\sqrt{(W^{-1})_{ii}}$ determines the value of the intersection of the ellipsoid with the corresponding i -parameter axis, and represents the one- σ bound on that parameter assuming all the others to be exactly known and equal to zero. Accordingly, with the R.H.S. of Eq. (27), the ellipsoidal surface constrains, at the 95% C.L. and model-independently, the range of values of the CI couplings $\epsilon_{\alpha\beta}$ allowed by the foreseen experimental uncertainties.

For the chosen input values for integrated luminosity, initial beam polarization, and corresponding systematic uncertainties, such model-independent limits are listed as lower bounds on the mass scales $\Lambda_{\alpha\beta}$ in Table 1.

All the numerical results exhibited in Table 1 can be represented graphically. In Figs. 1–3 we show the planar ellipses that are obtained by projecting onto the six planes $(\epsilon_{LL}, \epsilon_{LR})$, $(\epsilon_{LL}, \epsilon_{RL})$, $(\epsilon_{LL}, \epsilon_{RR})$, $(\epsilon_{RR}, \epsilon_{LR})$, $(\epsilon_{RR}, \epsilon_{RL})$, $(\epsilon_{LR}, \epsilon_{RL})$ the 95% C.L. allowed four-dimensional ellipsoid resulting from Eq. (27). In these figures, the inner and outer ellipses correspond to positron polarizations $|P_{\bar{e}}| = 0.6$ and $|P_{\bar{e}}| = 0.0$, respectively.

To appreciate the significant role of initial beam polarization we should consider that, in the unpolarized case the only available observables would be $\sigma_{\text{unpol}} \propto (\sigma_{LL} + \sigma_{RR}) + (\sigma_{LR} + \sigma_{RL})$ and $\sigma_{\text{unpol}} \cdot A_{\text{FB}} \propto (\sigma_{LL} + \sigma_{RR}) - (\sigma_{LR} + \sigma_{RL})$, see Eqs. (12) and (13). Therefore, by themselves, the pair of experimental observables σ_{unpol} and A_{FB} are not able to limit separately the CI couplings within finite ranges, but could only provide a constraint among the *linear combinations* of parameters $(\epsilon_{LL} + \epsilon_{RR})$ and $(\epsilon_{LR} + \epsilon_{RL})$. In some planes, specifically in the $(\epsilon_{LL}, \epsilon_{RR})$ and $(\epsilon_{LR}, \epsilon_{RL})$ planes, this constraint has the form of (unlimited) bands of allowed values, or correlations, such as those limited by the straight lines in Figs. 1–3. With initial beam polarization, two more physical observables become available, *i.e.*, A_{LR} and $A_{\text{LR,FB}}$, and this enables us to close the bands into the ellipses in Figs. 1–3. The allowed bounds obtained from the observables σ_{unpol} and A_{FB} are not affected by electron polarization (for unpolarized positrons). Therefore, the bounds in the form of straight lines are tangential to the outer ellipses referring to $P_{\bar{e}} = 0$, and in this case the role of $P_e \neq 0$ is just to close the corresponding band to a finite area.

Table 1: Reach in $\Lambda_{\alpha\beta}$ at 95% C.L., for the model-independent analysis performed in terms of conventional observables, for $e^+e^- \rightarrow \mu^+\mu^-$, $b\bar{b}$ and $c\bar{c}$ at $E_{\text{c.m.}} = 0.5$ TeV, $\mathcal{L}_{\text{int}} = 50 \text{ fb}^{-1}$ and 500 fb^{-1} , $|P_e| = 0.8$ and $|P_{\bar{e}}| = 0.0; 0.4; 0.6$.

$f\bar{f}$	\mathcal{L}_{int} fb^{-1}	Λ_{LL} TeV	Λ_{RR} TeV	Λ_{LR} TeV	Λ_{RL} TeV
$\mu^+\mu^-$	50	31.2; 33.9; 34.8	30.9; 33.9; 35.0	26.5; 29.4; 30.5	26.9; 29.9; 31.1
	500	46.1; 46.9; 46.8	47.0; 48.7; 48.7	45.8; 49.9; 51.3	46.5; 50.7; 52.0
$b\bar{b}$	50	37.0; 39.8; 40.8	33.0; 39.1; 41.4	25.2; 27.7; 28.7	31.8; 36.2; 37.9
	500	53.1; 54.0; 54.0	50.5; 63.9; 68.3	44.5; 48.8; 50.4	56.0; 63.3; 66.0
$c\bar{c}$	50	32.1; 34.7; 35.7	31.4; 35.4; 36.8	26.2; 28.8; 29.8	21.6; 24.5; 25.7
	500	47.6; 48.4; 48.4	50.0; 54.9; 55.6	45.7; 49.7; 51.2	38.1; 43.4; 45.5

While, in order to achieve this result, electron polarization is obviously essential, the results in Table 1 show that, at least in the kind of analysis presented here, the increase in the sensitivity to the parameters $\epsilon_{\alpha\beta}$ due to the additional availability of positron polarization is appreciable in most cases, but very modest or even absent in some, depending on the final $f\bar{f}$ channel and on the luminosity. This situation occurs in the cases, limited to the diagonal LL and RR combinations, where, with our chosen numerical input, the additional systematic uncertainty introduced by positron polarization competes with the statistical one. This is not the case for the non-diagonal combinations RL and LR, for which the statistical uncertainty remains the dominant one.

Furthermore, from the orientations of the ellipsis axes in Figs. 1–3, one can observe that in most considered cases the correlation among the different pairs of CI couplings is not so pronounced, but becomes somewhat more important at the higher value of the integrated luminosity. Clearly, from the strictly quantitative point of view, these features relate to the assumed input values for the systematic uncertainties.

The crosses in Figs. 1–3 represent the constraints obtainable by taking only one non-zero parameter at a time, instead of all four simultaneously non-zero, and independent, as in the analysis discussed here. Similar to the inner and outer ellipses, the shorter and longer arms of the crosses refer to positron polarization $|P_{\bar{e}}| = 0.6$ and 0.0 , respectively. Such ‘one-parameter’ results are derived from a χ^2 procedure applied to the combination of the four physical observables (12)–(15), also taking the above-mentioned correlations among observables into account.¹ As regards the role of polarization in this kind of single-parameter analysis, one finds that, basically, positron polarization in addition to electron polarization has more impact and generally allows an appreciable improvement of the sensitivity to CI couplings. Finally, one can note from Figs. 1–3 that the ‘single-parameter’ constraints on the individual CI parameters are numerically more stringent, as compared

¹This procedure leads to results numerically consistent with those presented from essentially the same set of observables in Ref. [23], if applied to the same experimental inputs used there.

to the model-independent ones. Essentially, this is a reflection of the smaller value of the critical χ^2 , $\chi^2_{\text{crit}} = 3.84$ corresponding to 95% C.L. with a *one-parameter* fit, and also of a reduced role of correlations.

On the other hand, as repeatedly emphasized in the Introduction, that procedure allows to test individual models corresponding to the parameter (or the combination of parameters) assumed to be non-zero, and in this sense it is model-dependent, whereas the allowed areas represented by the ellipses in Figs. 1–3 are model-independent. Actually, in this regard, one could compare the sensitivities shown in Table 1 (and Figs. 1–3) with the model-independent constraints on the parameters $\epsilon_{\alpha\beta}$ previously obtained using a set of polarized cross sections integrated in ‘optimal’ angular ranges as basic experimental observables [9–11]. One finds that, with few exceptions relevant to specific cases in the $b\bar{b}$ and $c\bar{c}$ sectors, although defining a somewhat more involved procedure the latter observables produce more stringent constraints compared to the simpler (and more practical) observables used here (mostly asymmetries). This is the combined effect of the relative numerical weights of statistical and systematical uncertainties input in the calculation, and of the optimization procedure introduced in [9–11]. In principle, further optimization of the asymmetries A_{FB} and $A_{\text{LR,FB}}$ may be possible.

Acknowledgements

This research has been supported by the Research Council of Norway, by MURST (Italian Ministry of University, Scientific Research and Technology) and by funds of the University of Trieste.

References

- [1] V. Barger, K. Cheung, K. Hagiwara and D. Zeppenfeld, Phys. Rev. D **57** (1998) 391 [hep-ph/9707412];
D. Zeppenfeld and K. Cheung, hep-ph/9810277;
K. Cheung, hep-ph/0106251.
- [2] G. Altarelli, J. Ellis, G. F. Giudice, S. Lola and M. L. Mangano, Nucl. Phys. B **506** (1997) 3 [hep-ph/9703276];
R. Casalbuoni, S. De Curtis, D. Dominici and R. Gatto, Phys. Lett. B **460** (1999) 135 [hep-ph/9905568].
- [3] E. Eichten, K. Lane and M. E. Peskin, Phys. Rev. Lett. **50** (1983) 811;
R. Rückl, Phys. Lett. B **129** (1983) 363.
- [4] D. Abbaneo *et al.* [ALEPH Collaboration], CERN-EP-2000-016.
- [5] A. F. Zarnecki, Eur. Phys. J. C **11** (1999) 539 [hep-ph/9904334].
- [6] A. F. Zarnecki, Nucl. Phys. Proc. Suppl. **79** (1999) 158 [hep-ph/9905565].
- [7] V. Barger and K. Cheung, Phys. Lett. B **480** (2000) 149 [hep-ph/0002259].

- [8] A. A. Pankov and N. Paver, Phys. Lett. B **432** (1998) 159 [hep-ph/9805207].
- [9] A. A. Babich, P. Osland, A. A. Pankov and N. Paver, Phys. Lett. B **476** (2000) 95 [hep-ph/9910403].
- [10] A. A. Babich, P. Osland, A. A. Pankov and N. Paver, Phys. Lett. B **481** (2000) 263 [hep-ph/0003253].
- [11] A. A. Babich, P. Osland, A. A. Pankov and N. Paver, LC Note LC-TH-2001-021 (2001), hep-ph/0101150.
- [12] B. Schrempp, F. Schrempp, N. Wermes and D. Zeppenfeld, Nucl. Phys. B **296** (1988) 1.
- [13] K. Flottmann, DESY-95-064; K. Fujii and T. Omori, KEK-PREPRINT-95-127.
- [14] S. Riemann, FORTRAN program ZEFIT Version 4.2;
D. Bardin et al., Comput. Phys. Commun. **133** (2001) 229 [hep-ph/9908433].
- [15] M. Consoli, W. Hollik and F. Jegerlehner, CERN-TH-5527-89 *Presented at Workshop on Z Physics at LEP*.
- [16] G. Altarelli, R. Casalbuoni, D. Dominici, F. Feruglio and R. Gatto, Nucl. Phys. B **342** (1990) 15.
- [17] A. Djouadi, A. Leike, T. Riemann, D. Schaile and C. Verzegnassi, Z. Phys. C **56** (1992) 289.
- [18] C. J. S. Damerell, D.J. Jackson, in *Proceedings of the 1996 DPF/DPB Summer Study on New Directions for High Energy Physics* (Snowmass 96), Edited by D.G. Cassel, L. Trindle Gennari, R.H. Siemann (SLAC, 1997) p. 442.
- [19] W.T. Eadie, D. Drijard, F.E. James, M. Roos, B. Sadoulet, *Statistical methods in experimental physics* (American Elsevier, 1971).
- [20] F. Cuypers and P. Gambino, Phys. Lett. B **388** (1996) 211 [hep-ph/9606391];
F. Cuypers, hep-ph/9611336.
- [21] D. E. Groom *et al.* [Particle Data Group Collaboration], Eur. Phys. J. C **15** (2000) 1.
- [22] F. James and M. Roos, Comput. Phys. Commun. **10** (1975) 343.
- [23] S. Riemann, LC Note LC-TH-2001-007 (2001).

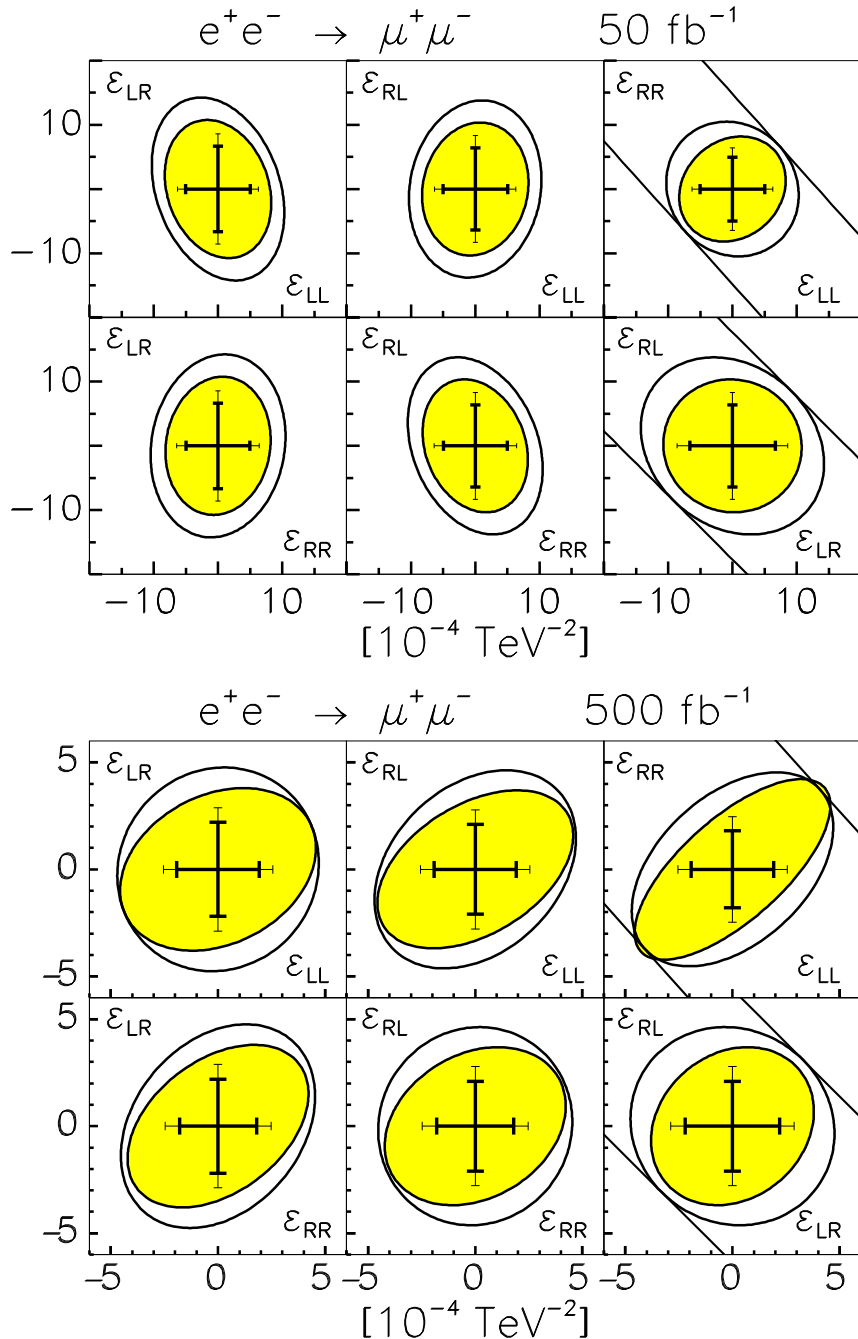


Figure 1: Two-dimensional projections of the 95% C.L. allowed region (27) for $e^+e^- \rightarrow \mu^+\mu^-$ at $\mathcal{L}_{\text{int}} = 50 \text{ fb}^{-1}$ and $\mathcal{L}_{\text{int}} = 500 \text{ fb}^{-1}$. Note that the scales are different. $|P_e| = 0.8$, $|P_{\bar{e}}| = 0.0$ (outer ellipse) and $|P_{\bar{e}}| = 0.6$ (inner ellipse). The solid crosses represent the ‘one-parameter’ bounds under the same conditions.

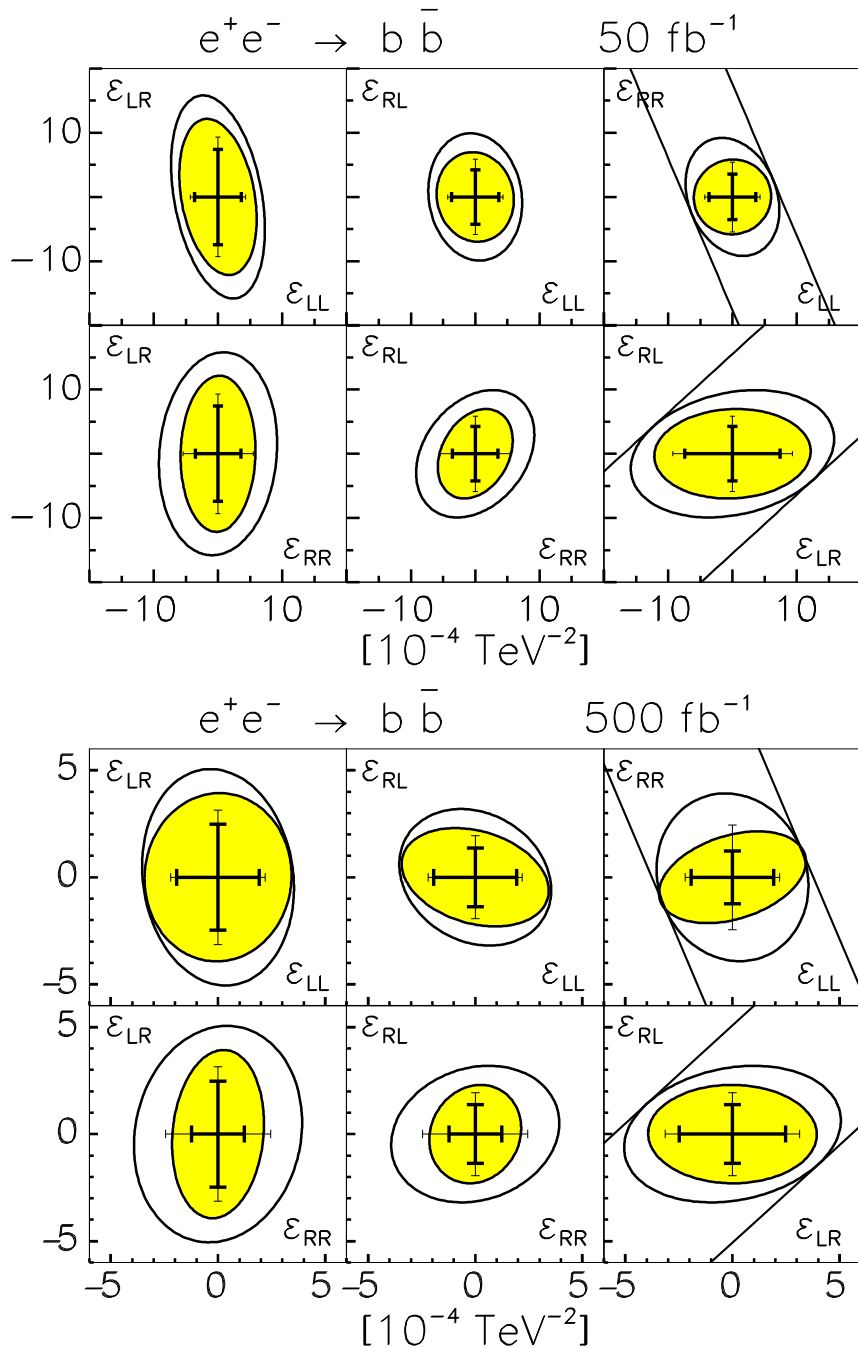


Figure 2: Same as Fig. 1, for the process $e^+e^- \rightarrow b\bar{b}$.

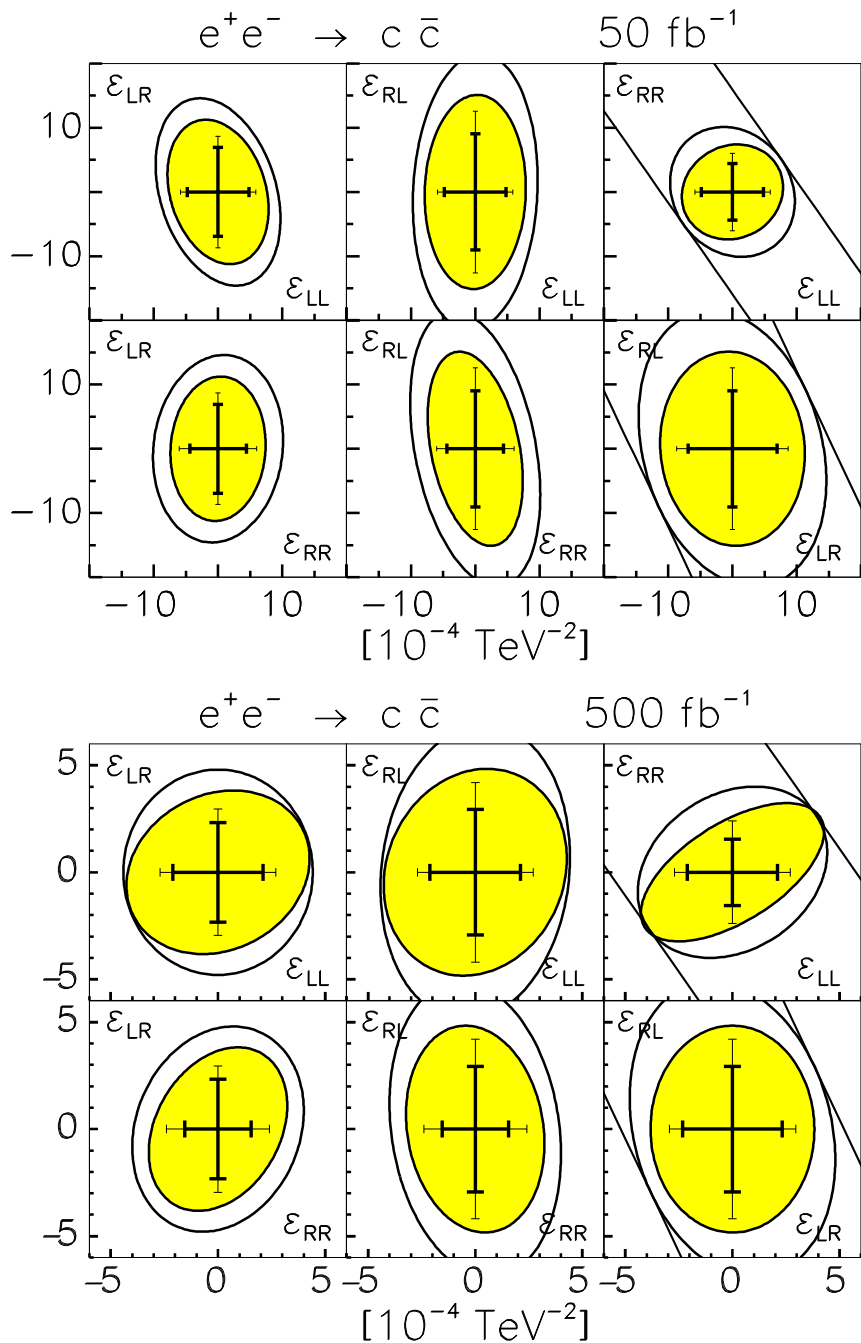


Figure 3: Same as in Fig. 1, for the process $e^+e^- \rightarrow c\bar{c}$.